THE JOURNAL OF PHYSICAL CHEMISTRY B

ARTICLE

pubs.acs.org/JPCB

On the Nature of Lithium Biphenyl in Ethereal Solvents. A Critical Analysis Unifying DFT Calculations, Physicochemical Data in Solution, and a X-ray Structure

Mónica de la Viuda, Miguel Yus, and Albert Guijarro*

Instituto de Síntesis Orgánica and Departamento de Química Orgánica, Universidad de Alicante, San Vicente del Raspeig, 03690 Alicante, Spain

Supporting Information

ABSTRACT: The lithium ion is an important type of electrolyte that has technological applications in the manufacture of lithium ion cells; therefore, a better understanding of the nature of its solutions is desirable. When associated to the radical anion of biphenyl in an organic solvent, it forms conducting solutions comparable to strong electrolytes such as lithium perchlorate. We have studied the lithium biphenyl solution in dimethoxyethane using DFT calculations. The nature of these ionic solutions is described in terms of a dynamic equilibrium between different types of ionic associations, the composition of which depends on the solvent and the temperature. The X-ray structure of $[Li^+ \cdot 4C_5H_{10}O][C_{12}H_{10}^{\bullet -}]$, a solvent-separated ion pair of lithium biphenyl complexed with tetrahydropyran, is reported. Its main structural characteristics coincide with the calculated one, which we think is the dominant species at room temperature, in agreement with the available physicochemical data.

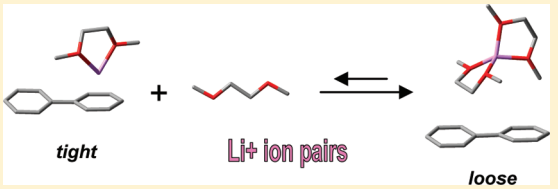

INTRODUCTION

Lithium ion cells are now widely used for portable electronic devices due to their small size, light weight, and high capacity.[1] They rely on the adequate migrating performance of Li^+ ions between the anode and the cathode through an organic electrolyte, which is generally composed of organic solvating mixtures. While the anode is formed from Li^+ intercalating compounds such as lithium graphite (LiC_6), the cathode is based on transition-metal compounds containing Li^+ (e.g., $LiCoO_2$, $LiMn_2O_4$, etc.), which release (uptake) Li^+ ions in charge (discharge) by changing the oxidation state of the transition metal. Among the different methods of chemical lithiation to prepare experimental cathodes, the use of lithium biphenyl solutions in DME was recently proposed.[2] On the other hand, mixtures of biphenyl and hexahydrobiphenyl are used in commercial lithium ion battery formulations as an overcharge protection agent,[3] enhancing their security by preventing smoke, flames, or explosions.[4] It seems thus important to acquire a solid knowledge of the nature of lithium-containing organic solutions, whether they are used for chemical synthesis or as electrolytes. In the course of our investigation on radical anions and dianions of policyclic aromatic hydrocarbons, we noticed the paper of H. Li et al., entitled *Li Biphenyl-1,2-dimethoxyethane Solution: Calculation and Its Application*",[2] which dealt with the nature of a Li biphenyl solution in DME. The authors tried to explain the nature of these intense blue solutions obtained by dissolving lithium metal in DME solutions of biphenyl. For that purpose, a theoretical study was published, consisting of a DFT study of the different species that they proposed to coexist in solution. The experimental data provided to back up these studies is scarce, mostly limited to the IR spectrum of a 1 M Li biphenyl solution in DME. The comparison of the IR absorptions with the calculated vibrational frequencies of the different species calculated by the authors was the main argument elicited to sustain the calculated structures. We believe that there are a number of scientific inconsistencies in these findings; therefore, we reconsidered the study in three fronts, (a) reproduction and reinterpretation of the DFT calculations, (b) account of the existing physicochemical data on these solutions, and (c) report of the first X-ray structure of a lithium biphenyl species. The purpose of this work is to provide a realistic description of the nature of the different species that exist in the lithium biphenyl solutions, in concordance with all of the available information on its properties, and we backed it up with experimental structural information.

ANTECEDENTS. ION PAIRING EQUILIBRIA OF LITHIUM BIPHENYL AND DILITHIUM BIPHENYL

Depending on the nature of the solvent, the counterion, and the temperature, radical anions and dianions of arenes, in general, and biphenyl, in particular, may exist as different entities that differ in the degree of association between the anionic and cationic parts of the molecule.[5] The nature of these species in solution has been better described as a dynamic model, which, for the case of lithium biphenyl (LiBP = $LiC_{12}H_{10}$), has been represented in Scheme 1. The different species of lithium biphenyl are

Received: August 4, 2011
Revised: October 14, 2011
Published: October 28, 2011

Scheme 1. Equilibrium Representing the Dynamic Model for Lithium Biphenyl in Solvating Media[a]

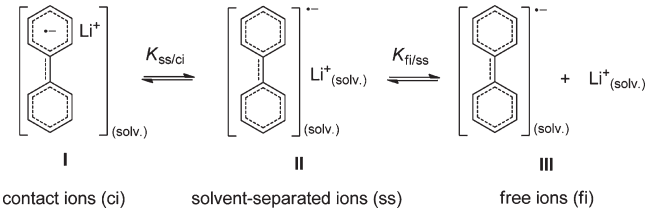

[a] Solvation of the ions increases as we move towards the right and decreases towards the left.

forming an equilibrium consisting of contact ion pairs (or tight, **I**) and solvent-separated ion pairs (or loose, **II**), from which free ions (**III**) can develop by further dissociation, although the concentration of free ions is normally low in low dielectric constant solvents. These equilibria are governed by a delicate thermodynamic balance that follows, in general, uniform trends regardless of the arene, and that is mainly governed by solvating effects. Solvating effects are quantified in terms of their enthalpic and entropic contributions. While generally $\Delta H^{\circ}_{(solv.)}$ is negative (exothermic), as we move toward the right in the whole equilibrium of Scheme 1 (due to the released heat of solvation), so is the $\Delta S^{\circ}_{(solv.)}$, which sees its value diminish as an increased number of solvent molecules are captured at their fixed coordination sites (provoking a loss of entropy in the solvation process). The overall effect is a temperature-dependent equilibrium that shifts to the left (i.e., in the direction free → loose → contact ion pairs) as the temperature is increased and vice versa, that is, it shifts toward the right (contact → loose → free ion pairs) as the temperature is lowered.[6] The radical anion of biphenyl is not an exception to this general scenario.[7] Concerning the cation, Li^+ has the highest enthalpy of solvation among alkaline cations due to its smaller size, favoring loose ion pairs over tight pairs in the ion pairing equilibrium in coordinating solvents.[8] The effect of the solvent is well known too.[5c,d] The solvating power of different ether solvents toward alkali salts of biphenyl was determined by inspection of the alkali NMR chemical shifts at varying temperatures.[9] For ^{6}Li and ^{7}Li NMR (as well as for other alkali cations), the solvating power was established as DME > THF > THP (1,2-dimethoxyethane, tetrahydrofuran, and tetrahydropyran, respectively), as expected. In a very relevant part of this study, the degree of association of LiBP (**I** ⇆ **II** in Scheme 1) could be directly inferred from experimental data. Interestingly, for lithium biphenyl (~0.94 M) in DME, the plot of the ^{7}Li NMR chemical shift data versus T (temperature) displays a positive slope at high T that levels off at about ~25 °C. Lower than that, there is a flat (zero) dependence with T, indicating that below that temperature, nearly all of the molecules of lithium biphenyl are fully dissociated into solvent-separated ion pairs (**I** → **II**), and the contribution of the Fermi contact from **I** to the ^{7}Li NMR chemical shift vanishes below this point. In THF, the same overall effect is observed, although at slightly lower temperatures as a consequence of its somewhat less solvating power. This has been corroborated by another report[10] in which the contribution of the Fermi contact shifts to the solutions of LiBP in THF in a similar range of concentrations (~1 M) was concluded to be very small, indicating that the solution was chiefly dominated by loose ion pairs (only THF at 300 K was studied). The available information indicates that the solution of lithium biphenyl in DME is overwhelmingly dominated by **II** already at 25 °C. This makes it difficult to calculate the equilibrium constant $K_{ss/ci}$ and thermodynamic parameters $\Delta H^{\circ}_{(ss/ci)}$ and $\Delta S^{\circ}_{(ss/ci)}$ of the first equilibrium in Scheme 1 given the high reactivity of the lithium biphenyl toward the solvent at higher temperatures, where the contact pair concentration would grow in importance. The same problems were reported for the less reactive and structurally related 9-fluorenyl lithium ($LiC_{13}H_9$). It has a higher ratio of contact ions given its higher degree of charge localization. Still, it was reported as ~100% solvent-separated ion pairs in DME at 25 °C but ~80% solvent-separated and 20% contact ion pairs in THF at the same temperature based on their UV spectra, with an approximate $\Delta H^{\circ}_{(ss/ci)} = -7$ kcal mol^{-1}, while $\Delta S^{\circ}_{(ss/ci)}$ could not be determined accurately.[5a,b] Let us move now to the second equilibrium in Scheme 1 (**II** ⇆ **III**). In general, ionic species are mainly associated into ion pairs in low dielectric constant solvents ($\varepsilon_r < 10-15$).[11] In ether solvents, the solvent-separated ion pairs are dissociated into free ions only to a small extent. Still, it is possible to distinguish between free ions (e.g., **III**) and associated ions (e.g., **II** or **I**) by conductivity measurements because only free ions are responsible for electrical conductivity in solution. From there, the dissociation constants of associated into free ions, K_{diss}, can be obtained. Strictly speaking, $K_{diss} = [fi]/([ci] + [ss])$, that is, the direct dissociation into free ions both from contact and solvent-separated ions is to be accounted for, although in our case, this is simplified because the concentration of contact ions can be neglected, $[ci] \ll [ss]$; then, $K_{diss} \approx K_{fi/ss} = [fi]/[ss]$. The equilibrium between nonconducting paired ions and free ions was studied for lithium biphenyl in THF, affording a $K_{diss} = 4.2 \times 10^{-6}$ M at 25 °C. $\Delta H^{\circ}_{(diss)} = -2.5$ kcal mol^{-1} and $\Delta S^{\circ}_{(diss)} = -33$ cal mol^{-1} K^{-1} were also determined for this process at 25 °C from experiments of limiting molar conductance (Λ_0).[12] Again, these values are comparable to those of 9-fluorenyllithium in THF, with $K_{diss} = 3.9 \times 10^{-6}$ M at 25 °C, $\Delta H^{\circ}_{(diss)} = -3.2$ kcal mol^{-1}, and $\Delta S^{\circ}_{(diss)} = -35.5$ cal mol^{-1} K^{-1}, obtained in the same way.[13] These data point toward a very small concentration of free ions in the lithium biphenyl solutions in DME at 25 °C,[11] which is completely negligible concerning a interpretation of the IR spectrum of the solution. Another important piece of information emerging from these studies is that the formation of higher aggregates does not seem to be important for the lithium biphenyl radical anion (as well as for other alkali ions) in coordinating ether solvents.[12]

In the presence of an excess of $Li_{(s)}$, the scenario shown above is insufficient to describe the nature of these deep blue solutions. The high reduction potential of $Li_{(s)}$ in coordinating solvents[14] allows access to extremely reduced species, that is, the dianion of biphenyl (Li_2BP). We have observed that under certain conditions and in the presence of an excess of $Li_{(s)}$, LiBP is overreduced to some extent to the dianion Li_2BP, which displays specific reactivity patterns absent for the radical anion LiBP.[15] The actual structure of Li_2BP (tentatively represented as **IV**) is so far unknown by experimental means but is anticipated to be a robust contact triple ion in ether solvents even at low temperatures as the result of strengthened Coulombic interactions.[7a,16] We have recently observed this experimentally in the case of naphthalene (NP). The structure of solvent-separated ion pair of the radical anion (LiNP) turns into a robust contact triple ion as it is further

Table 1. Total Energies (E), Zero-Point Vibrational Energy (ZPE), and Free Energies ($\Delta G°$) of the Different Species Related to the Reaction of Li and BP in DME, as Proposed in Ref 2 and This Work[a]

	data from ref 2			this work			
chemical species	E(Ha)	ZPE(Ha)	$\Delta G°$ (kJ mol^{-1})	E(Ha)	ZPE (Ha)	$\Delta G°$ (Ha)	point group
Li	−7.4913			−7.4913	0	−7.5047	
Li^+	−7.2849			−7.2849	0	−7.2977	
BP (**1**)	−463.2387	0.1808		−463.2387	0.1808	−463.2706	D_{2h}[b]
BP (**2**)				−463.2421	0.1808	−463.2754	D_2
LiBP (**3**)	−470.7505	0.1793	−33.2	−470.7505	0.1793	−470.7880	C_s
LiBP (**4**)[c]	−470.7440	0.1798	−13.9				
$Li^+BP^{\bullet-}$ (**5**)	−470.7505	0.1793	−560.9[d]	−470.7505	0.1793	−470.7880	C_s[e]
LiBP·DME (**6**)	*f*			−779.6039	0.3222	−779.6543	C_1
LiBP·DME (**7**)	*f*			−779.5939	0.3218	−779.6467	C_1
$BP^{\bullet-}$ (**8**)	−463.2435	0.1749	−15.98	−463.2435	0.1749	−463.2766	D_{2h}[g]
$BP^{\bullet-}$ (**9**)				−463.2434	0.1751	−463.2797	D_2[g]
BP^{-2} (**10**)	−463.1209	0.1814	305.96	−463.1250	0.1791	−463.1586	C_{2h}[h]
Li_2BP (**11**)	−478.2636	0.1800	−87.4	−478.2758	0.1799	−478.3137	C_{2h}
Li_2BP (**12**)	−478.2600	0.1797	−70.0	−478.2725	0.1804	−478.3093	C_{2v}[i]
$LiBP^-$ (**13**)	−470.7612	0.1776	−43.4	−470.7611	0.1777	−470.7977	C_s
DME (**14**)	−308.8142	0.1407		−308.8143	0.1406	−308.8461	C_{2h}
DME (**15**)				−308.8136	0.1406	−308.8453	C_2[j]
Li^+·DME (**16**)	−316.1014	0.1455	−197.6	−316.1987	0.1447	−316.2310	C_2
Li^+·DME (**17**)	−316.1617	0.1428	−136.7	−316.1617	0.1428	−316.1964	C_1
Li^+·2DME (**18**)				−625.0742	0.2878	−625.1212	S_4[k]
$[Li^+·2DME][BP^{\bullet-}]$ (**19**)				−1088.4204	0.4649	−1088.4851	C_1[l]

[a] From DFT theory, the B3LYP/6-311++G(d,p) level was used for all minimization and single-point calculations throughout the table. Energies in Hartrees, except for $\Delta G°$ from ref 2, which was reported as relative values in kJ mol^{-1}. The total energies E include the ZPE vibrational corrections. Free energies ($\Delta G°$ of the molecule/atom from elementary particles) are calculated at 298.15 K and 1 atm. BP = biphenyl, DME = 1,2-dimethoxyethane. Structures **1**−**19** are drawn in Charts 1 and 2. [b] Compound **1** (D_{2h}) has one imaginary frequency; the true minimum is **2** (D_2). [c] One imaginary frequency, reported by the authors. [d] Odd data (see text and Scheme 2). [e] Structures **5** and **3** are identical. [f] No numerical data; only a drawing was reported. [g] Structures **8** and **9** are nearly identical in energy; structure **8** (D_{2h}) has one imaginary frequency, while **9** (D_2) is a true minimum. [h] Isolated dianion; it is unstable toward e^- dissociation and yields unrealistic data (see text). [i] Also possible with lower symmetries (C_2, C_1) and very close geometries and energies. [j] Corresponding to the synclinal conformation, somewhat less populated than the antiperiplanar **14**. [k] Also possible with lower symmetry (C_1) and similar energy and geometry. [l] Corresponds to the structure of an average solvent-separated ion pair.

reduced to the dianion (Li_2NP). Both were charachterized by X-rays.[17]

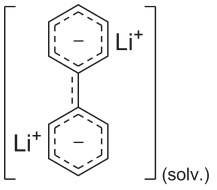

IV

COMPUTATIONAL DETAILS

Density functional theory calculations (DFT)[18] of neutral and ionic structures, energies, and harmonic vibrational analysis of lithium biphenyl were carried out using the Becke−Lee−Yang−Parr (B3LYP) exchange−correlation functional[19] in order to reproduce the energies reported by the authors in Table 1. The geometries of the isolated neutral and ionic species have been optimized in the gas phase using the 6-311++G (d,p) basis set.[20] The calculations are therefore identical to those reported by Liu et al.[2] Analytic second-derivative calculations, which yield the harmonic frequencies, were performed on the optimized geometries at the same level of theory to ensure that the optimized geometries are true minima on the hypersurface of potential energy and to provide corrections for the zero-point energy (ZPE) effects. The Hessian matrices of the optimized geometries have only positive eigenvalues, whereas a transition structure gives rise to a one negative eigenvalue. The calculations were carried out with the Gaussian 03 suite of programs.[21] Graphic material was drawn with Chimera[22] and Mercury.[23]

EXPERIMENTAL SECTION

Preparation of crystals of $[Li^+·4C_5H_{10}O][\ C_{12}H_{10}^{\bullet-}]$: A 30 mm round-bottom tube was loaded with lithium powder ($Li_{(s)}$ 99%, Aldrich, 10 mmol, ∼70 mg)[15d] and biphenyl (Aldrich, >99%, 4 mmol, 623 mg) under Ar atmosphere. The tube was filled with freshly distilled THP (10 mL, distilled from NaK alloy) and was sonicated (40 kHz, 360 W) for 30 min at room temperature. The dark-colored suspension obtained was allowed to rest for 72 h at 3 °C. The supernatant solution and lithium excess were removed and replaced by mineral oil (previously dried and deoxygenated by gently shaking with NaK alloy under an Ar atmosphere). Inspection of the resulting crystalline mass allowed the selection of appropriate monocrystals that were submitted to X-ray difraction analysis. Crystal data for $[Li^+·4C_5H_{10}O][\ C_{12}H_{10}^{\bullet-}]$: $C_{20}H_{40}LiO_4·C_{12}H_{10}$, M = 505.678 g mol^{-1}, monoclinic,

Chart 1. Calculated Structures 1−10 and Symmetry Point Group, As Described in Table *1*

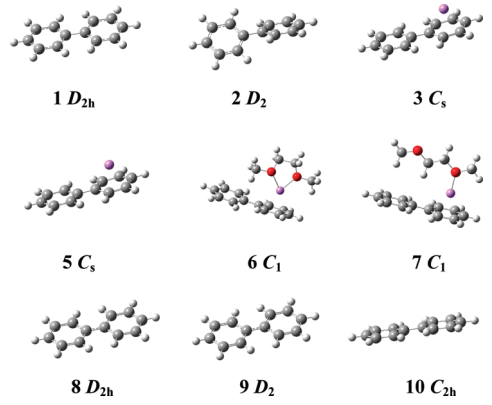

Chart 2. Calculated Structures 11−19 and Symmetry Point Group, As Described in Table *1*

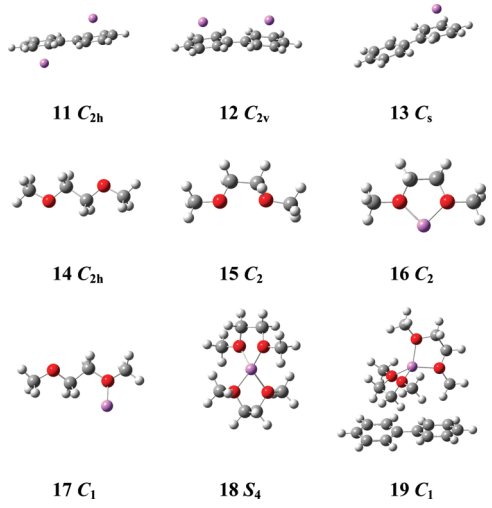

a = 19.191(2), b = 9.8248(11), c = 17.327(2) Å, β = 110.442(2)°, V = 3061.2(6) Å^3, T = 173(1) K, space group $C2/c$, $\rho_{(calc)}$ = 1.097 g cm^{-3}, Z = 4, λ = 0.71073 Å, μ = 0.069 mm^{-1}, 12510 reflections collected, 2720 independent reflections. R_{int} = 0.0430. Final $wR2$ = 0.1166 for all data and 168 parameters; R_1 = 0.0444 for 1762 $F_o > 4\sigma(F_o)$.

RESULTS AND DISCUSSION

In the following sections, we shall try to provide a reasonable picture of the nature of the different species **I**−**IV** that exist in solutions of lithium biphenyl by mean of DFT calculations and comment on the above-reported structural data obtained by X-ray diffraction.

(a). Reinterpretation of the DFT Calculations and Search for the Chemical Species That Occur in Lithium Biphenyl in DME. Table 1 collects a recent attempt to describe the structure of the different chemical species in the LiBP solution with DME as a solvent by means of DFT calculations (columns on the left).[2] We have repeated the most relevant elements of that study and provided a complete set of data for comparison and analysis (Table 1, columns on the right and Supporting Information).

Scheme 2. Calculated Thermodynamic Free-Energy Cycle Showing the Formation of Lithium Biphenyl from Li and BP (Biphenyl)[a]

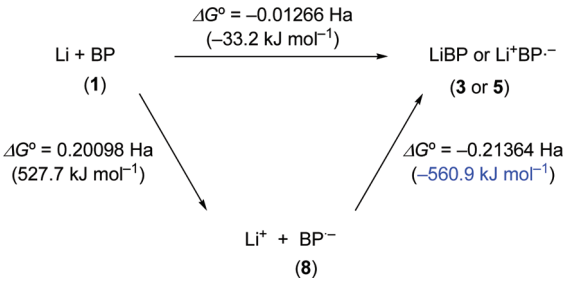

[a] LiBP (**3**) and Li$^+$BP$^{\bullet-}$ (**5**) are identical structures, regardless of the route drawn to reach them. Data from Table 1.

The first discrepancy comes from the biphenyl itself (**1**), which is reported as having a D_{2h} symmetry, that is, a torsion angle between phenyls of 0°. A closer look at the repeated calculation of **1** reveals that to be a saddle point with one imaginary frequency. **1** is flanked by two degenerated torsional conformers **2** of lower symmetry (D_2), which are true minima and have a torsional angle (dihedral) of 41.1° between both phenyls.[24] This is in fair agreement with the experimental gas-phase electron diffraction data value of 44.4° at 401 K.[25]

Structure **3** (LiBP) corresponds to the non solvated contact ion pair, and it is a key issue in our discussion. Notice that the structure **3** is identical to the structure **5** (Li$^+$BP$^{\bullet-}$), for which a large $\Delta G°$ = −560.9 kJ mol^{-1} was reported, despite the identical energies between **3** and **5** (E = −470.7505 Ha). The explanation for this apparent incongruence came from a careful evaluation of the free energies involved in the process by means of a Bordwell thermodynamic cycle. The corresponding ion pair can be reached by two ways. These are (a) reaction of neutral lithium and biphenyl, Li + BP → LiBP, which is the actual synthetic protocol, and (b) combination of the ions into a contact pair, Li$^+$ + BP$^{\bullet-}$ → LiBP. Route (b) can be hypothesized, but only after an electron transfer step between reagents, Li + BP → Li$^+$ + BP$^{\bullet-}$. This electron transfer step was overlooked in the former study of the reaction and prompted the authors to propose the ion pair formation on the basis the highly exergonic character of step (b), which is especially so when calculated in the gas phase ($\Delta G°$ = −560.9 kJ mol^{-1}).[2] The two routes are summarized in Scheme 2.

The following step is expected to be the solvation of the ion pairs by DME. Structures **6** and **7** represent solvated ion pairs as proposed in the literature.[2] No energy data were reported on either **6** or **7**, but from the drawn structures, the calculation could be completed and the energies reported (Table 1, compounds **6** and **7**, columns on the right). Both **6** and **7** are reported as contributing to the experimental IR spectrum of a 1 M solution of lithium biphenyl in DME at room temperature. The calculated equilibrium **6** ⇆ **7** ($\Delta G°$ = +19.9 kJ mol^{-1}, $K_{298.15}$ = 3 × 10^{-4}), however, points toward an overwhelming prevalence of the double- over the single-coordinated form, as is otherwise expected. Although **6** appears to us as a reasonable first approach to the structure of the contact ion pair **I** of Scheme 1, experimental studies on the lithium biphenyl solutions in DME at 25 °C show that the contact ion pair is not the dominant species, as mentioned before.

We shall focus now on isolated charged species. The radical anion BP$^{\bullet-}$ appears to have two possible structures, **8** and **9**, very

dx.doi.org/10.1021/jp2074573 |J. Phys. Chem. B 2011, 115, 14610–14616

close (practically nondiscernible) in energy. Tightening the convergence criteria,[26] a flat D_{2h} geometry is found (**8**). A more detailed look to the potential energy surface reveals this to be a saddle point flanked by two identical true minima of slightly lower free energy and D_2 symmetry (**9**) that are torsional conformers (dihedral = 1.4°).[27]

Isolated dianion **10** was evaluated only for comparison purposes. We found a lower-energy minimum than that reported (Table 1, **10**, columns on the left and on the right). Still, the most relevant point in here is a different one. Most dianions in the gas phase are unstable toward dissociation of their outermost electrons (e.g., **9** has its HOMO electrons in a b_u orbital of +0.13 Ha). It has been already described that without stabilizing effects (e.g., of Li^+), the tendency of high-energy electrons to escape from the dianion leads to large, abnormal coefficients for several diffuse functions in the HOMO, yielding meaningless information.[15c]

In the synthetic procedure described in ref 2, equimolar amounts of $Li_{(s)}$ and biphenyl were used. This, in principle, limits the formation of dianionic species in solution, which would be relegated only to the highly unfavorable equilibrium of disproportionation of the radical anion, $2LiBP \leftrightarrows Li_2BP + BP$.[28] Still, three structures of lithium salts of the biphenyl dianion were reported, **10** (C_{2h}), **11** (C_{2v}), and **12** (C_s). Li_2BP **10** has both lithium ions in opposite faces of the molecule (or anti).[29] It is the most stable isomer, compared to the *syn*-Li_2BP isomer **11** (**10** $\leftrightarrows$ **11**, ΔG° = +11.5 kJ mol^{-1}). The participation of a partially dissociated salt such as $LiBP^-$ **12** is equally unlikely given, in addition to the former arguments, the strong tendency of dianions to form tight contact triple ions.[7a]

Solvation of the cation is crucial for the reaction to proceed at all.[5c] DME has several thermally accessible conformations. **14** (C_{2h}) corresponds to the antiperiplanar one, the most stable. Only 2 kJ mol^{-1} above in free energy, the synclinal **15** (C_2) is another relative minimum that occurs as a pair of degenerate conformers. All are part of the conformational equilibrium of the solvent.

In the case of the solvated lithium cation, $Li^+ \cdot$DME **16** and **17**, we found again some inconsistencies. As in the case mentioned above, **16** and **17** are reported as contributing to the experimental IR spectrum. The energy and geometry of monocoordinated **17** (C_1) match exactly with those from our calculations. However, a substantially lower energy was found for **16** (C_2), which, otherwise, looks like a more probable structure compared to **17**. Contrary to the former report, we found that the dicoordinated compound **16** is by far a more stable complex. On the basis of the calculated equilibrium **16** $\leftrightarrows$ **17**, ΔG° = +90.8 kJ mol^{-1}, $K_{298.15} = 1.2 \times 10^{-16}$, it is clear that monocoordinated **17** should not account for the spectroscopic properties of the mixture. H. Li et al. mentioned the occurrence of a strong IR band at 556 cm^{-1} after the dissolution of lithium.[2] This absorption was attributed to the stretching of Li^+ bound to oxygen of **17** (related to the ν_{12} B vibrational mode), which is only compatible with the prevalence of a monocoordinated form in the mixture, as well as to the analogous stretching of **7** (related to the ν_{28} A vibrational mode), which is also unlikely to be substantially populated.

Given the strong tendency of lithium for completing its coordination sphere, the occurrence of dicoordinated **16** itself is also questionable in solutions of DME. We have considered full solvation of the Li^+ by DME. The complex $Li^+ \cdot 2$DME **18** (S_4) has two DME molecules coordinating one Li^+ ion in a pseudotetrahedral environment with an overall S_4 symmetry. The equilibrium **16** + DME $\leftrightarrows$ **18**, $\Delta G^\circ = -115.9$ kJ mol^{-1}, $K_{298.15} = 2 \cdot 10$,[20]

Scheme 3. Equilibrium between the Contact Ion Pair (6) and the Solvent-Separated Ion Pair (19) As the Most Representatives Species of LiBP in DME[a]

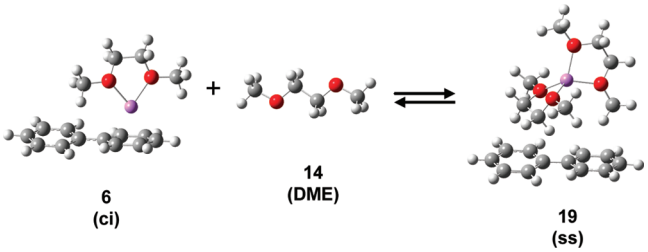

[a] The equilibrium shifts towards close contact **6** as the temperature rises and towards solvent-separated **19** as the temperature lowers.

is illustrative (DME = **14**). The dicoordinated compound **16** itself is strongly destabilized compared to **18** in DME and is not expected to contribute to the properties of the mixture.

Finally, because the available experimental data suggest the prevalence of solvent-separated ion pairs, we have tried to simulate the structure of **II** in Scheme 1. Ion pair $[Li^+ \cdot 2DME][BP^{\bullet -}]$ **19** was obtained as a local minimum. Extensive screening of different initial orientations of its forming ions **18** and **9** gave **19** recurrently as the most stable structure. With no intention of being rigorous, we were tempted to reproduce the complexation equilibria that involve close contact ion pair **6** and solvent-separated ion pair **19** in DME using the reported calculations, that is, the first equilibrium in Scheme 1. Lets consider the equilibrium between contact (**6**) and solvent-separated (**19**) ion pairs in DME, LiBP·DME(**6**) + DME(**14**) $\leftrightarrows$ $[Li^+ \cdot 2DME][BP^{\bullet -}]$(**19**). Interestingly, this turned out to be a temperature-dependent equilibrium, shifted to solvent-separated ion pairs at low temperatures and to contact ion pairs at higher temperatures. For the reaction at 0 K, the free energy of the reaction can be equated to the total energy (including the ZPE), $\Delta G^\circ_{0K} = \Delta E = -5.8$ kJ mol^{-1}, favoring the solvent-separated ion pair. Instead, at higher temperature (298.15K), the same equilibrium is shifted toward the contact ion, ΔG° = +40.1 kJ mol^{-1}. This highlights opposite and compensating effects of the enthalpic and entropic contributions of the solvating process, which gives rise to a temperature-dependent equilibrium (the calculated values are $\Delta H^\circ = -4.2$ kJ mol^{-1} and $\Delta S^\circ = -149$ J mol^{-1} K^{-1} at 298.15K) (Scheme 3). Aware of the inherent incapability of gas-phase calculations to reproduce exactly the complexity of the experimental solvation phenomena, we discarded further studies such as a temperature study of the equilibrium or further attempts to get a better fit of the thermodynamic constant at room temperature.[30] Still, were very pleased to find a temperature-dependent behavior that fit qualitatively the experimental trends displayed with the temperature.

(b). Crystal Structure of Lithium Biphenyl Coordinated with Tetrahydropyran, $[Li^+ \cdot 4THP][BP^{\bullet -}]$. In order to complete the description of this important reagent, precise structural data in the solid state would be highly desirable. We initially tried to obtain the X-ray structure of the ion pair $[Li^+ \cdot 2DME][BP^{\bullet -}]$ to compare its general structural parameters to the calculated one (**19**), but the lack of adequate quality in the crystals prevented this goal. After several trials with different solvents and conditions, the complex of lithium biphenyl in THP afforded the required crystals. It is interesting to notice that the solvent for crystallization was THP, a less coordinating solvent in which

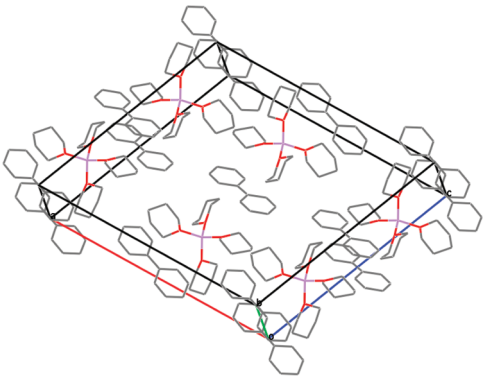

Figure 1. Monoclinic unit cell composed of biphenyl radical anions [$BP^{\bullet-}$] and lithium cations coordinated with four molecules of THP [$Li^+ \cdot 4THP$]. It displays an internal structure composed of four symmetry-equivalent molecules ($Z = 4$) of [$Li^+ \cdot 4C_5H_{10}O$][$C_{12}H_{10}^{\bullet-}$]. Hydrogen atoms have been omitted for clarity.

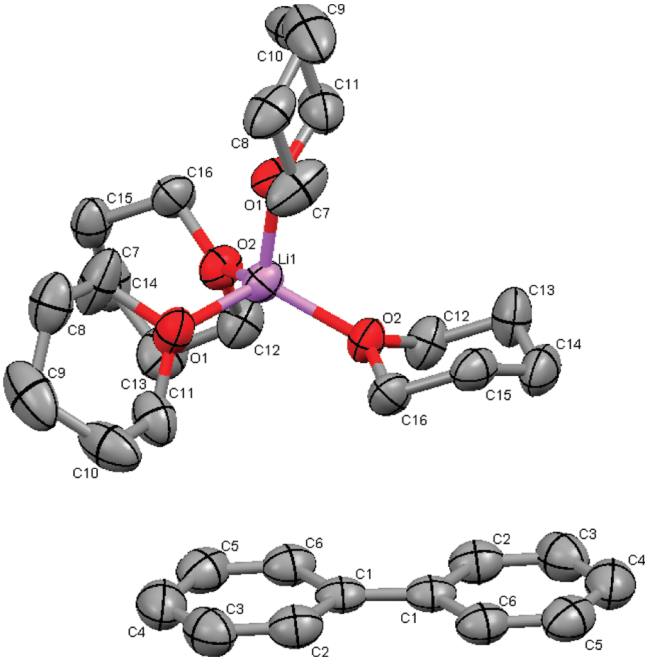

Figure 2. Isolated [$Li^+ \cdot 4C_5H_{10}O$][$C_{12}H_{10}^{\bullet-}$] molecule from the crystal, showing the structure of a solvent-separated ion pair. Symmetry transformation used to generate equivalent atoms in [$Li^+ \cdot 4C_5H_{10}O$]: $-x, -1 + y, 1/2 - z$; in [$C_{12}H_{10}^{\bullet-}$]: $-x, -y, -z$. Thermal ellipsoids are shown at the 50% probability level. Hydrogen atoms have been omitted for clarity.

close contact ions are actually observed by EPR.[31] Despite that, it is the solvent-separated ion pair and not the contact ion pair that crystallizes. The crystal unit cell of [$Li^+ \cdot 4THP$][$BP^{\bullet-}$] is represented in Figure 1. It belongs to the $C2/c$ space group of the monoclinic system. Each naked biphenyl radical anion is equidistantly located in between two lithium cations, which themselves are coordinated with four molecules of THP. This is characteristic of an ionic interaction. Figure 2 is one isolated molecule from the crystal, obtained by choosing one [$BP^{\bullet-}$] and the closest-facing coordinated cation [$Li^+ \cdot 4THP$]. There is a pseudotetrahedral coordination around the lithium cation by the four THP molecules, which are themselves in a typical chair conformation. The isolated biphenyl subunit is nearly flat. It has an actual C_i symmetry, presumably imposed by the packing forces within the crystal. The two phenyl rings are contained in parallel plains separated by only ~0.1 Å and exchange by a local inversion center. Still, the symmetry is very close to C_{2h} or even higher such as D_2 or D_{2h} if the geometrical constraints are slightly loosened, reproducing thus well the geometries of the radical anion in the gas phase (**8** and **9**).[32,33] We shall compare now the structures of the calculated **19** and experimental solvent-separated ion pairs. The distance from Li^+ to the biphenyl centroid in the crystal is 5.42 ± 0.02 Å,[33] which is the closest distance between the geometric center of the anion and the closest cation. As a comparison, the same distance measured for structure **19** was 4.98 ± 0.02 Å.[34] A difference is expected because the Li^+ is centered above the biphenyl centroid in **19**, and it is not necessarily so in the crystal due to the effect of crystalline tensors. However, if we look at the distance from the Li^+ to the biphenyl least-squares plane, it turns out to be very close in both structures, 4.91 ± 0.02 Å in the crystal and 4.94 ± 0.02 Å in calculated **19** (see Figures S1−S4 in Supporting Information for drawings and measurements). The coordination shell of Li^+ is similar in both cases, despite the structural differences, and therefore, it is the stabilizing effect on the anion. For all of the above-mentioned reasons, we think that **19** is a fair approach to represent the average solvent-separated ion pair in an isotropic medium as DME.

CONCLUSIONS

In summary, the identity of the main chemical species that form the solutions of lithium biphenyl in DME has been addressed. The general scenario is described by a subtle equilibrium between close contact, solvent-separated, and, to a lesser extent, free ions, which is described by its corresponding thermodynamic relationships. Structural and thermodynamic information on the system was obtained by means of DFT calculations; these results replace former theoretical interpretations that overlooked full coordination of the Li^+ ion. Calculations afford a temperature-dependent equilibrium between close contact and solvent-separated ions that reproduces qualitatively the behavior of the system. Experimentally, the weight of each type of ion in the equilibrium depends on the solvating properties of the solvent and the temperature. For the case of DME, the solution is fully dominated by solvent-separated ions at room temperature. Finally, the experimental X-ray structure of a solvent-separated ion pair of lithium biphenyl complexed with THP is provided, and its structural characteristics in comparison with the calculated one in DME are discussed.

ASSOCIATED CONTENT

Supporting Information. Detailed information on X-ray diffraction data collection, including the crystallographic information file (cif). Figures with distance measurements of ion pairs S1−S4. Calculation geometries and energies of compounds **1**−**19** from Table 1. This material is available free of charge via the Internet at http://pubs.acs.org.

AUTHOR INFORMATION

Corresponding Author

*Fax: (+34) 965-90-35-49. E-mail: aguijarro@ua.es.

■ ACKNOWLEDGMENT

This work was generously supported by the Spanish Ministerio de Educación y Ciencia [CTQ2011-24165, CTQ2007-65218, and CONSOLIDER INGENIO 2010 (CSD2007-00006)], the Generalitat Valenciana (PROMETEO 2009/039), and the Universidad de Alicante.

■ REFERENCES

(1) Yoshio, M.; Brodd, R. J.; Akiya, K. Introduction. In *Lithium-Ion Batteries: Science and Technologies*; Yoshio, M.; Brodd, R. J.; Akiya, K., Eds.; Springer Science+Business Media: New York, 2009; pp xvii−xxvi.

(2) Liu, N.; Li, H.; Jiang, J.; Huang, X.; Chen, L. *J. Phys. Chem. B* **2006**, *110*, 10341–10347.

(3) Ue, M. Role Assigned Electrolytes: Additives. In *Lithium-Ion Batteries: Science and Technologies*; Yoshio, M.; Brodd, R. J.; Akiya, K., Eds.; Springer Science+Business Media: New York, 2009; pp 96−101.

(4) Xiao, F.; Wang, M.; Zhou, G.; You, H. *Type of Mixed Additives and Electrolyte for Lithium-Ion Secondary Batteries Using such Mixed Additives*. U.S. Patent 2007/0105021 A1, May 10, 2007.

(5) (a) Hogen-Esch, T. E.; Smid, J. *J. Am. Chem. Soc.* **1965**, *87*, 669–670. (b) Hogen-Esch, T. E. Smid. *J. Am. Chem. Soc.* **1966**, *88*, 307–318. (c) Shatenshtein, A. I.; Petrov, E. S. *Russ. Chem. Rev.* **1967**, *36*, 100–110. (d) Holy, N. L. *Chem. Rev.* **1974**, *74*, 243–277.

(6) The magnitude of this effect is larger at the first stage of the dissociation (**I** ⇆ **II** in Scheme 1) which is more exothermic.

(7) (a) Buschow, K. H. J.; Dieleman, J.; Hoijtink, G. J. *J. Chem. Phys.* **1965**, *42*, 1993–1999. For a remark on this paper, see ref 16.

(8) Indeed, the pair $Li_{(s)}/Li^{+}_{(H2O)}$ is the most negative among alkali metals, with a standard potential of $E°(Li/Li^{+})$ = −3.04 V in water relative to SHE; see: *CRC Handbook of Chemistry and Physics*, 85th ed.; CRC Press: Boca Raton, FL, 2004; pp 8−33.

(9) Canters, G. W.; de Boer, E. *Mol. Phys.* **1973**, *26*, 1185–1198.

(10) Micha-Screttas, M.; Heteropoulos, G. A.; Steele, B. R. *J. Chem. Soc., Perkin Trans. 2* **1999**, 1443–1446.

(11) For example, 1,2-dimethoxyethane, $\varepsilon_{r\ (DME)}$ = 7.22, and tetrahydrofuran, $\varepsilon_{r\ (THF)}$ = 7.58 at 25°C; see: *CRC Handbook of Chemistry and Physics*, 89th ed. (internet version); CRC Press/Taylor and Francis: Boca Raton, FL, 2009.

(12) Nicholls, D.; Sutphen, C.; Szwarc, M. *J. Phys. Chem.* **1968**, *72*, 1021–1027.

(13) Hogen-Esch, T. E.; Smid, J. *J. Am. Chem. Soc.* **1966**, *88*, 318–324.

(14) For reduction potentials of Li metal, see: (a) A reported half-peak potential for the pair $Li_{(s)}/Li^{+}_{(THF)}$ is found, $E_{1/2}$ (Li/Li^{+}) = −3.07 V, in THF/$LiBPh_4$ versus Ag/AgCl, see: Mortensen, J.; Heinze, J. *Tetrahedron Lett.* **1985**, *26*, 415–418. (b) The formal $Li_{(s)}/Li^{+}_{(THF)}$ potencial in THF was measured recently, E_{0f} = −3.48 V versus $Fc/Fc^{+}PF_6^{-}$; see:Paddon, C. A.; Ward Jones, S. E.; Bhatti, F. L.; Donohoe, T. J.; Compton, R. G. *J. Phys. Org. Chem.* **2007**, *20*, 677–684.

(15) (a) Perez, H.; Melero, C.; Guijarro, A.; Yus, M. *Tetrahedron* **2009**, *65*, 10769–10783. (b) Melero, C.; Perez, H.; Guijarro, A.; Yus, M. *Tetrahedron Lett.* **2007**, *48*, 4105–4109. (c) Melero, C.; Guijarro, A.; Baumann, V.; Perez-Jimenez, A. J.; Yus, M. *Eur. J. Org. Chem.* **2007**, 5514–5526. (d) Melero, C.; Herrera, R. P.; Guijarro, A.; Yus, M. *Chem.—Eur. J.* **2007**, *13*, 10096–10107.

(16) Slates, R. V.; Szwarc, M. *J. Phys. Chem.* **1965**, *69*, 4124–4131.

(17) Melero, C.; Guijarro, A.; Yus, M. *Dalton Trans.* **2009**, 1286–1289.

(18) (a) Hohenberg, P.; Kohn, W. *Phys. Rev.* **1964**, *136*, B864–B871. (b) Kohn, W.; Sham, L. *Phys. Rev.* **1965**, *140*, A1133–A1138.

(19) (a) Becke, A. D. *J. Chem. Phys.* **1993**, *98*, 5648–5652. (b) Stephens, P. J.; Devlin, F. J.; Chablowski, C. F.; Frisch, M. J. *J. Phys. Chem.* **1994**, *98*, 11623–11627.

(20) Krishnan, R.; Binkley, J. S.; Seeger, R.; Pople, J. A. *J. Chem. Phys.* **1980**, *72*, 650–654.

(21) Frisch, M. J.; Trucks, G. W.; Schlegel, H. B.; Scuseria, G. E.; Robb, M. A.; Cheeseman, J. R.; Montgomery, J. A. Jr.; Vreven, T.; Kudin, K. N.; Burant, J. C. et al. *Gaussian 03*, revision D.01; Gaussian, Inc.: Wallingford, CT, 2004.

(22) *UCSF Chimera version 1.5.3*. http://www.cgl.ucsf.edu/chimera (2011).

(23) *Mercury version 2.4.6*. http://www.ccdc.cam.ac.uk/mercury/ (2011).

(24) For an exhaustive study on biphenyl and its conformations reaching the same conclusions as those here, see:Sancho-García, J. C.; Cornil, J. *J. Chem. Theory Comput* **2005**, *1*, 581–589.

(25) Almenningen, A.; Bastiansen, O.; Fernholt, L.; Cyvin, B. N.; Cyvin, S. J.; Samdal, S. *J. Mol. Struct.* **1985**, *128*, 59–76.

(26) The SCF convergence criteria were set to 10^{-8} Hartree on the density (SCF=Tight) as well as the convergence of geometric optimizations [OPT=tight: maximum force and root-mean-square (rms) force of 3×10^{-6} and $<1 \times 10^{-7}$ Hartree $Bohr^{-1}$, respectively, and maximum and rms displacements of 1.4×10^{-5} and 3×10^{-6} Bohr, respectively]. A pruned grid having 99 radial shells and 590 angular points per shell was used in both cases (INT=UltraFine).

(27) A new, more accurated set of energies (Ha) is obtained for **8** (D_{2h}): E = −463.2433, ZPE = 0.1750, $\Delta G°$ = −463.2765; **9** (D_2): E = −463.2433, ZPE = 0.1751, $\Delta G°$ = −463.2794.

(28) An estimate of this K_{dispr} can be obtained from the first ($E°_1$ = −2.68 V) and second reduction potentials ($E°_2$ = −2.68 V) of biphenyl; $\ln K_{dispr} = nF(E°_2 - E°_1)/RT$; $K_{dispr} = 3.5 \times 10^{-9}$; see:Meerholz, K.; Heinze, J. *J. Am. Chem. Soc.* **1989**, *111*, 2325–2326.

(29) For other calculated Li_2BP, see:Irle, S.; Lischka, H. *J. Mol. Struct.: THEOCHEM* **1996**, *364*, 15–31.

(30) In that respect, notice that the anion $B^{\bullet-}$ remains essentially unsolvated in **19**; solvation of this anion should give a larger, more negative enthalpy of reaction (both from the energy of solvation as well as from the *PV* work) and presumably a better fit at room temperature.

(31) Hyperfine splittings due to the $^{7}Li^{+}$ (a = 0.136 G) were observed for lithium biphenyl in THP at room temperature; see: Nishiguchi, H.; Nakai, Y.; Nakamura, K.; Ishizu, K.; Deguchi, Y.; Takakia, H. *Mol. Phys.* **1965**, *9*, 153–161.

(32) The comparison of the C−C bond distances in Å of $[BP^{\bullet-}]$ between the crystal and structures **8** or **9** reveals only slight differences ranging from 0.6 to 1.9% (with always shorter bonds in the crystal). The crystallographic esd (estimated standard deviation) of $[BP^{\bullet-}]$ in the crystal is already 0.7−0.8% for the same bonds. (Notice that bond distances in **8** and **9** are statistically identical within these errors.)

(33) Calculated from the crystallographic esd at the 99.7% confidence level.

(34) Error expressed as the mean-squared deviation for the computational method and basis set used when applied to the determination of bond distances; see:Sánchez, J.; Fernández, M. *J. Mol. Struct.: THEOCHEM* **2003**, *624*, 239–249.